

Diffusion weighted imaging of the breast at 7T – ready for clinical application?

Olga Zarić¹, Katja Pinker², Stephan Gruber³, David Porter³, Thomas Helbich², Siegfried Trattig¹, and Wolfgang Bogner^{1,4}

¹MR Centre of Excellence, Department of Radiology, Medical University of Vienna, Wien, Wien, Austria, ²Department of Radiology, Medical University of Vienna, Wien, Wien, Austria, ³MR PLM AW Neurology, Siemens Healthcare, Erlangen, Germany, ⁴Athinoula A. Martinos Center for Biomedical Imaging, Department of Radiology, Massachusetts General Hospital, Harvard Medical School, Boston, Massachusetts, United States

Target Audience:

Scientists with interest in 7T clinical application of DWI and breast MRI.

Purpose:

So far there is only one preliminary study on a few subjects that were examined by diffusion weighted imaging (DWI) of the breast at 7T and which illustrates the feasibility of DWI at ultra-high magnetic fields with significantly increased signal-to-noise ratios (SNR)[1]. However, in this previous study only unilateral MRI was performed using a standard single-shot echo planar imaging (ssEPI) sequence. This limits both the spatial coverage and possible spatial resolution that can be obtained even if a lot of SNR is available. At 7T, shorter T_2 of breast tissue, higher Larmor frequency, and increased magnetic field inhomogeneities lead to stronger T_2^* blurring, increased spatial distortions and spatially inhomogeneous fat suppression. At 3T, the use of parallel imaging (PI)[2] and readout-segmented EPI (rsEPI)[3] independently reduced blurring and distortions in breast DWI. Improved B1-insensitive fat suppression additionally enhanced image quality [3]. In our study we evaluated, if an efficient combination of rsEPI, PI and improved fat suppression can provide reproducible high-resolution bilateral DWI data for clinical evaluation of breast lesions at 7T.

Methods:

Phantom and *in vivo* measurements were performed on a 7T Magnetom Scanner (Siemens, Erlangen, Germany) using a bilateral double tuned $^31\text{P}/^1\text{H}$ 4-channel breast coil (Stark, Erlangen, Germany). IRB approval and written, informed consent were obtained. 31 consecutive patients with 33 histopathologically verified breast lesions (20 IDC, 1 ILC, 1 DCIS, 8 fibroadenoma and 2 benign papilloma) were included in this study. In phantoms, DWI by ssEPI and rsEPI with/without PI and comparable imaging parameters was performed to evaluate differences in imaging artifacts and to optimize imaging parameters. In patients, only rsEPI (9 readout segments) with PI (factor 2) was used: three-scan trace diffusion schema; Stejskal-Tanner diffusion; $b=0$ & 850 s/mm^2 ; fat suppression by combined frequency selective saturation & gradient reversal technique; semi-automatic shimming; TR/TE=5500/65 ms; resolution $0.9 \times 0.9 \times 5 \text{mm}^3$; matrix 170×340 ; 28 slices; echo spacing 0.34 ms; TA 3:48 min.

The image quality was evaluated visually and SNR values and contrast-to-noise ratios (CNR) of lesions were quantified. Regions of interest (ROIs) were drawn in all lesions (23 malignant (mean size $2.3 \pm 0.2 \text{cm}$) and 10 benign (mean size $1.8 \pm 0.3 \text{cm}$)) and in the contralateral normal breast parenchyma to investigate differences in the apparent diffusion coefficient (ADC). The diagnostic accuracy was calculated based on an ADC threshold obtained from ROC curve analysis.

Results:

All 31 DWI examinations of the breast at 7T achieved reproducible good image quality. No data had to be excluded from evaluation. Phantom measurements showed that combination of rsEPI and PI reduced the amount of blurring and geometric distortions by a factor of 3.4 compared to standard ssEPI with PI and even a factor of 6.9 compared to ssEPI without PI. This improvement provided *in vivo* DWI data with excellent anatomical correlation compared to T1-weighted reference MRI data (Fig. 1). Both, spatial resolution and contrast of DWI with $b=0$ s/mm^2 was similar to that normally reached by additional STIR images. However, low B1 sensitivity near the chest, particularly near the axilla would have inhibited the evaluation of lesions in this region.

The average SNR for $b=0$ s/mm^2 measured in normal glandular breast tissue, benign, and malignant tissue was 32 ± 13 , 104 ± 44 and 42 ± 16 , respectively ($p < 0.005$). The CNR of benign lesions (2.1 ± 0.2) was 40% higher than for malignant lesions (1.5 ± 0.3) ($p < 0.005$).

There were significant differences between the ADC values for all tissue types ($p < .001$) (Fig.2). Excellent differentiation of lesions was found based on ADC values (in mean \pm standard deviation $\times 10^{-3} \text{mm}^2/\text{s}$): 0.98 ± 0.19 for malignant and 1.88 ± 0.41 for benign lesions. A diagnostic accuracy of 100% was found when using an ADC threshold of $1.35 \times 10^{-3} \text{mm}^2/\text{s}$.

Discussion:

Our study provides the first clinical evidence that the efficient combination of rsEPI and PI for DWI examinations of the breast overcomes restrictions in spatial resolution and provides reproducible high-quality DWI data for diagnostic use even at 7T. Future improvements in coil technology and B1 shimming techniques will further improve image quality by correcting for B1 inhomogeneities near the axilla and close to the chest. Since ADC maps are derived from two images with identical B1 effects, ADC maps were significantly less affected by B1 inhomogeneities than DWI itself.

Conclusions:

At 7T, DWI of the breast with submillimeter inplane resolution provided exceptional image quality leading to excellent differentiation of benign and malignant breast lesions.

Fig. 1: Sample DWI and reference images obtained at 7T from a 72 years old patient with a high-grade invasive ductal carcinoma with necrotic center. High resolution ($0.9 \times 0.9 \text{mm}$ inplane) DWI with minimal geometric distortions or blurring and excellent fat suppression enable excellent delineation of the malignant border compared to the necrotic center of the lesion: (A) DWI ($b=850 \text{mm}^2/\text{s}$); (B) T1-weighted contrast enhanced MRI; (C) ADC map; (D) DWI ($b=0 \text{mm}^2/\text{s}$).

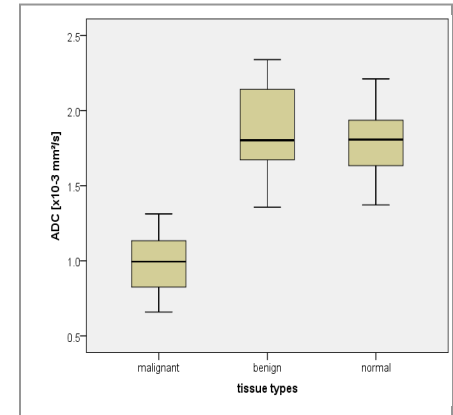
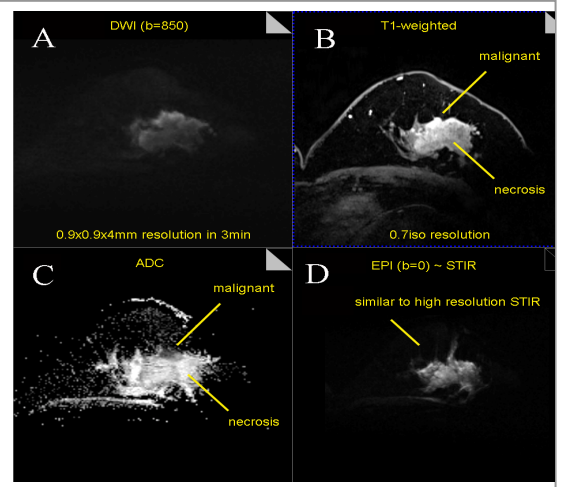


Fig. 2: Boxplot diagram shows differentiation of tissue types (malignant, benign and normal) on basis of ADCs calculated from combined b-value protocol of 0 and $850 \text{mm}^2/\text{s}$. A diagnostic accuracy of 100% was achieved using an ADC threshold level of $1.35 \times 10^{-3} \text{mm}^2/\text{s}$.

References:

- [1] Korteweg et al. Invest Radiol 2011 Jun;46(6):370-6
- [2] Kuroki et al. Magn Reson Med Sci 2004;3(2):79-85
- [3] Bogner et al. Radiology. 2012 Apr;263(1):64-76